

VISUALIZATION OF FC72 CONFINED NUCLEATE BOILING

Júlio César Passos

Eduardo Ludgero da Silva

Luís Felipe Bastiani Possamai

Department of Mechanical Engineering

LABSOLAR/NCTS

Federal University of Santa Catarina

88040-900 Florianópolis-SC-Brazil

jpssos@emc.ufsc.br

Abstract. This paper presents a new visualization study for confined and unconfined boiling of FC72 at atmospheric pressure and low and moderate heat fluxes ($\leq 40 \text{ kW/m}^2$) on a downward facing disc placed at 0.2, 0.5, 1 and 13 mm distance from the base of a boiling chamber. The results show that boiling for $s=0.2$ and 0.5 mm can be considered enhanced compared with $s=1$ and 13 mm. Still photographs of the boiling phenomenon showed the coexistence of isolated and coalesced bubbles for $s \geq 0.5$ mm and the predominance of deformed coalesced bubbles for $s=0.2$ and 0.5 mm.

Keywords: nucleate boiling, Bond number, confined boiling, heat transfer, visualization

1. INTRODUCTION

Boiling in micro and mini channels is of practical interest in microelectronics cooling because of the high heat flux to be removed from individual chips, Nowell et al. (1995). The search for compact equipment which can work under conditions of high heat flux, employing boiling as the main heat transfer mechanism, has led to increasing interest in studies on boiling in narrow channels. For a narrow vertical channel consisting of the annulus between a glass tube and an internal heated cylinder, Ishibashi and Nishikawa (1969) showed the existence of two main mechanisms: isolated bubbles for low heat flux or moderate confinement and coalesced and deformed bubbles for high heat flux or high confinement.

Figure 1a shows a schematic representation of a vapor bubble in an unconfined space and the corresponding contact angle θ that decreases when the bubble is confined and deformed in a narrow channel as represented in Fig. 1b. Several theoretical analyses have demonstrated the important role



Figure 1. Scheme showing the contact angle for: a) a quasi-spherical bubble,
b) a deformed (flattened) bubble

of the evaporation of the liquid film in the region between the wall and the bubble, understood to be the bubble area pressed against on the heated wall, which is called the microlayer (Carey, 1992;

Stephan, 1992; Dhir, 1996). For the confined configuration represented in Fig. 1b the thickness of the microlayer becomes thinner than in the case of (a) and the bubble area pressed against the heated wall is increased, which contributes to the enhancement of boiling in narrow channels. As was experimentally shown by Katto et al. (1977) this enhancement effect tends to decrease when the heat flux is relatively high.

A simple way to analyze the degree of confinement is to compute the Bond number, Bo , defined as the ratio between a characteristic dimension of the confined space, s , and the capillary length, L , this latter being proportional to the vapor bubble departure diameter and calculated by :

$$L = \sqrt{\frac{\sigma}{g(\rho_l - \rho_v)}} \quad (1)$$

where g , σ , ρ_l and ρ_v represent the acceleration due to gravity, the surface tension and the densities of the liquid and the vapor, respectively. The Bond number is $Bo=s/L$. As a general trend, when the confined characteristic dimensions decrease, the heat transfer coefficient increases (Ishibashi and Nishikawa, 1969 ; Katto et al., 1977 ; Yao and Chang, 1983; Passos et al., 2004a,b). When the order of magnitude of the Bond number is less than unity there is a tendency to have coalesced bubbles whereas for $Bo>1$ the bubbles are isolated. However, for $Bo<1$, the boiling crisis is characterized by dryout which may be highly dependent on the confinement and occurs for heat fluxes that decrease with a decrease in s or Bo as reported by Katto et al. (1977), Yao and Chang (1983), Bonjour and Lallemand (1997) and Geisler and Bar-Cohen (2003). Depending on the geometry and confinement the dryout heat flux can be of the same order of magnitude as the desired heat flux of operation, Passos et al. (2004b).

The bubble departure diameter, d_d , can be calculated using the following equation, as recommended by Carey (1992):

$$d_d = 0.0208\theta L \quad (2)$$

where θ represents the contact angle and L is the capillary length, Eq.(1).

Séméria (1964) presented photographs of the boiling phenomenon taken by stereoscopy and a high speed camera of 5000 frames/s and showed the hydrodynamic effect caused by the departure of bubbles from isolated nucleation sites. A more complex phenomenon characterizes the boiling heat and mass transfers for higher heat flux due to the interaction between phenomena at micro and macro scales. Katto et al. (1977) filmed, with a high speed camera, the boiling of distilled water in a narrow channel whose the heated surface was an upward facing copper disk of 11 mm diameter. The successive photographs presented by Katto et al. (1977) show changes in the liquid-vapor configuration, for a nucleate boiling regime and $s=0.5$ mm, corresponding to a Bond number of 0.2, at intervals of 3.2 and 5.4 ms. The authors attributed the enhancement of nucleate boiling for the cases corresponding to a Bond number less than unity to the evaporation of an extremely thin static liquid film on the heated surface at the bubble bottom. The evaporation of a thin liquid film on the heating surface at the bubble bottom had been previously postulated by Ishibashi and Nishikawa (1969). The visualization study of the FC72 boiling in confined and unconfined spaces, Passos et al. (2004b), even when the liquid is subcooled, showed coalesced bubbles blanketing most of the heating copper disc, when the distance (s) between the heating disc and the bottom base is 0.2 and 0.5 mm, corresponding to Bond numbers of 0.28 and 0.69, for heat fluxes higher than 25 kW/m^2 . For subcooled boiling and s values of 1 and 13 mm, corresponding to Bond numbers 1.38 and 17.95, and a heat flux equal to or less than 40 kW/m^2 , the bubbles were isolated with a small number of large bubbles when $s=1$ mm.

This paper presents new experimental results on the thermal behavior and still photographs for the confined boiling of FC72 in a narrow space and in wider spaces, between a downward facing

heating disc and the base of the boiling chamber. A selection of 39 pictures extracted from 584 pictures and distributed among nine ensembles are presented.

2. EXPERIMENTAL SET UP

The test section is a copper disc with a diameter of 12 mm and thickness of 1 mm with three E thermocouples of 0.15 mm diameter set in it, close to the centre of the disc, one of them being a differential type of thermocouple, and heated by an 15.9Ω electrical resistance skin heater fixed to the upperside of the disc. The copper disc is fixed to a piece of PVC with a diameter 20 mm and this is mounted onto the end of an aluminium tube which the thermocouple cables pass through. The test section is mounted inside a boiling chamber, consisting of a glass tube with a 50 mm inside diameter and filled with a dielectric liquid, FC72. Another two thermocouples are installed inside the boiling chamber. The boiling chamber is mounted inside a second chamber, 150x150x160 mm, as shown in Figure 2, with water flowing inside whose temperature is controlled by a cryostat allowing the control of the temperature of the working fluid. The distance between the base of the boiling chamber and the copper disc is adjustable by turning the aluminium tube and controlling the distance by means of a dial indicator.

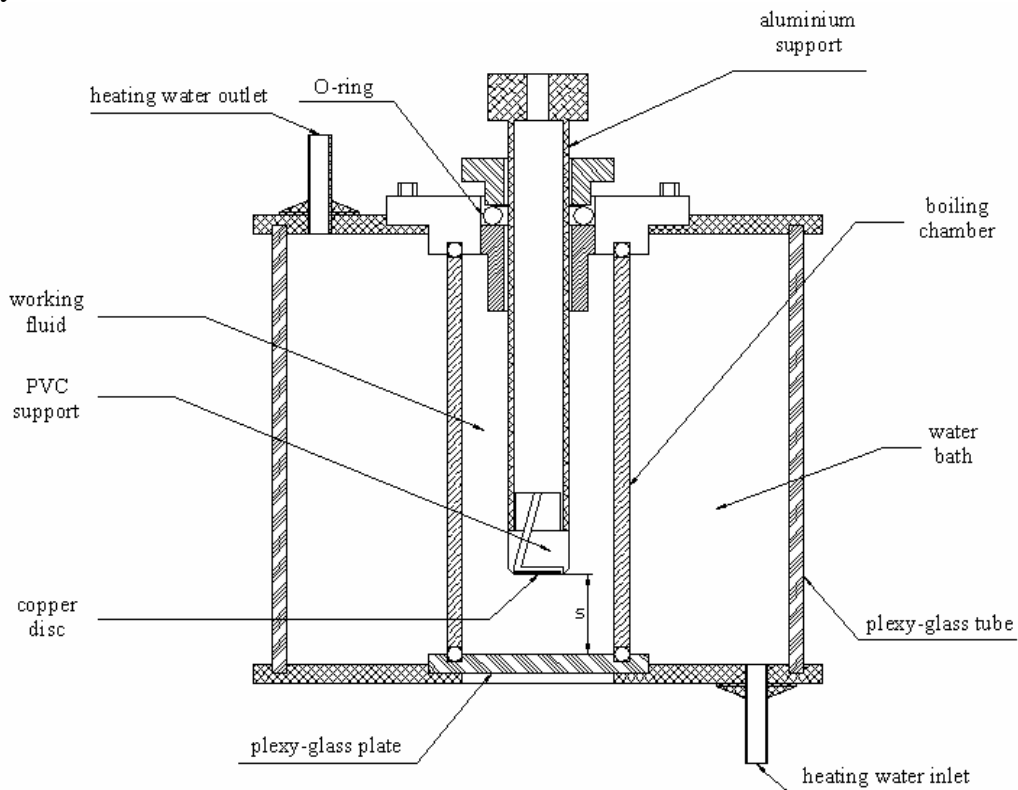


Figure 2. Scheme of the experimental set up

The heating disc is downward facing. The base of the boiling chamber is transparent and allows the visualisation of the boiling phenomenon. The copper surface in contact with the working fluid was polished using emery paper #600, corresponding to a roughness R_p of $1.1 \mu\text{m}$. The tests were performed in an FC72 pool, at atmospheric pressure, at LABSOLAR/ NCTS of the Federal University of Santa Catarina, in Brazil. Still photographs of the boiling phenomenon was taken from the bottom of the test section with a digital camera CANON EOS Rebel 6.3 Megapixel with a lens EF-S 18-55 mm, f 3.5-5.6.

A DC power supply, HP6030A, is connected to the skin heater and controlled by a PC using LABVIEW and the prior data acquisition and treatment are carried out by a HP34970A. The heating of the disc is controlled by increasing or decreasing the heat flux.

2.1. Experimental Procedure

The experimental procedure is programmed in LABVIEW and each average experimental point, defined by a wall temperature and a heat flux, represents a 90 s duration in the increasing mode of heating and 420 s in the decreasing mode of heating.

The temperature uncertainty was $\pm 0.6^\circ\text{C}$, using the same procedure reported by Passos and Reinaldo (2000). The experimental uncertainty for the heat flux was 1%, and those for the heat transfer coefficients varied from 3 to 7% and were computed following the procedure presented by Holman (1989) and Kline (1985).

3. RESULTS

The departure diameter calculated using Eq. (2), for a contact angle of 45° , and the physical properties of FC72, furnishes $d_d=0.75\text{mm}$, and the Bond number, as referred in the introduction, was 0.28 and 0.69 for the distances of 0.2 and 0.5 mm, respectively. Equation (2) is also valid for upward facing heating systems, see Carey (1992), and this value of d_d indicates a trend for $s=0.2$ and 0.5 mm towards confined boiling.

Figures 3a-c show the effect of confinement for s values of 0.2, 0.5 and 1 mm for heat fluxes of 20, 30 and 40 kW/m^2 . For each of these three values of heat flux we can verify that the liquid-vapour interface configurations for $s=0.2\text{ mm}$ and $s=1\text{ mm}$ are very different. For $s=1\text{ mm}$ ($Bo=1.38$) there is a predominance of individual bubbles that in some cases can be covered by large coalesced bubbles, Figures 3a-c. In some photographs, for $s=1\text{ mm}$, it seems that there are small bubbles covered by the large bubbles, the latter escaping through the periphery of the test section as shown in Figs. 3a-c. For $s=0.2\text{ mm}$ the vapour-liquid interface configuration shows the predominance of a large vapour film, the area of which increases with increasing heat flux. For the intermediate distance, $s=0.5\text{ mm}$, we can observe the coexistence of large flattened bubbles with some small bubbles whose numbers decrease by the coalescence phenomenon, when the heat flux increases. The temperature values given under the photographs show that the wall temperatures for $s=0.2$ and 0.5 mm and heat fluxes of 20 and 30 kW/m^2 are less than that for $s=1\text{ mm}$, which indicates the enhanced boiling phenomenon for Bond numbers less than unity when the heat flux is low or moderate. In the third case, $q=30\text{ kW/m}^2$, the wall temperature for $s=0.2\text{ mm}$, is higher than for the others two distances and the dryout phenomenon is occurring. The photograph for this latter case shows that the majority of the plate surface is dry.

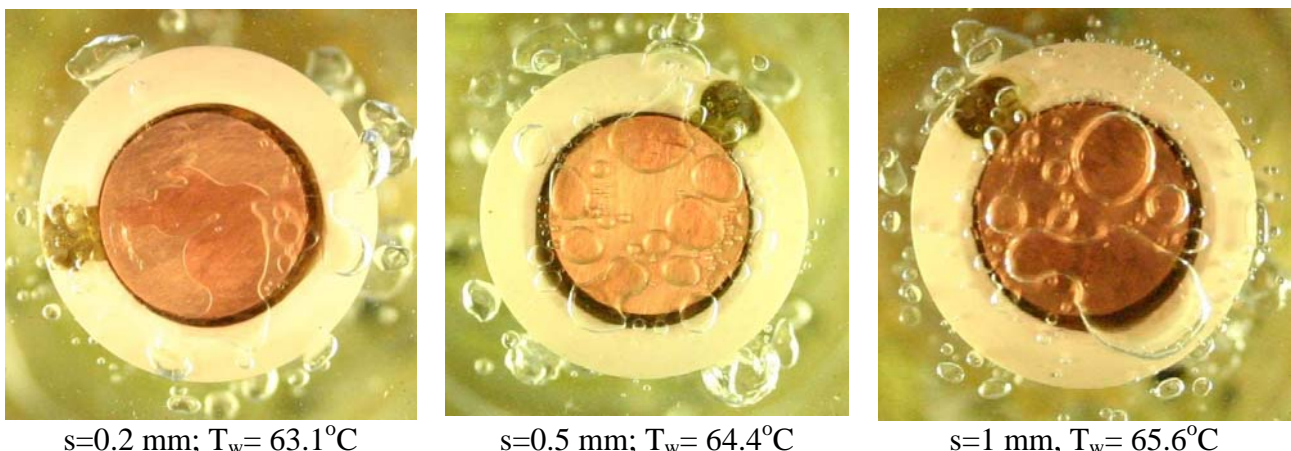
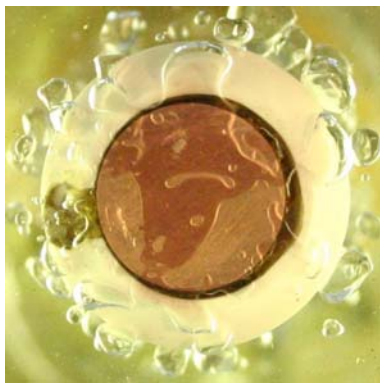


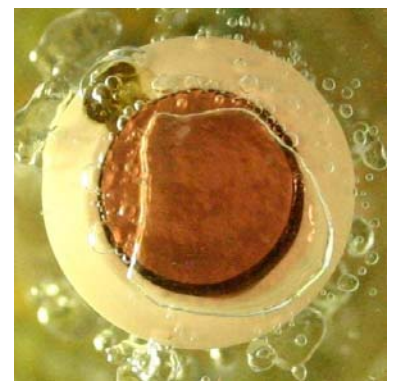
Figure 3a. Effect of confinement for a heat flux of 20 kW/m^2



$s=0.2 \text{ mm}; T_w= 66.0^\circ\text{C}$

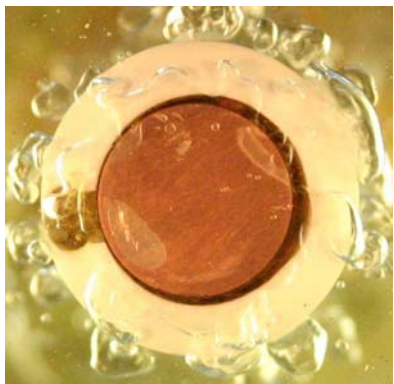


$s=0.5 \text{ mm}; T_w= 66.2^\circ\text{C}$



$s=1 \text{ mm}; T_w= 67.4^\circ\text{C}$

Figure 3b. Effect of confinement for a heat flux of 30 kW/m^2



$s=0.2 \text{ mm}, T_w= 75.5^\circ\text{C}$



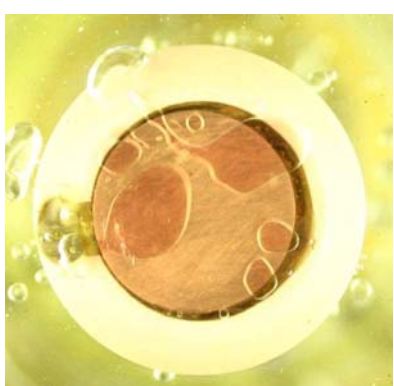
$s=0.5 \text{ mm}, T_w= 68.1^\circ\text{C}$



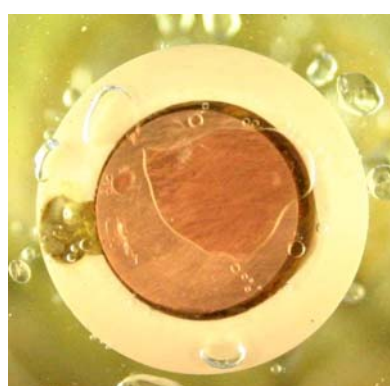
$s=1 \text{ mm}, T_w= 69.3^\circ\text{C}$

Figure 3c. Effect of confinement for a heat flux of 40 kW/m^2

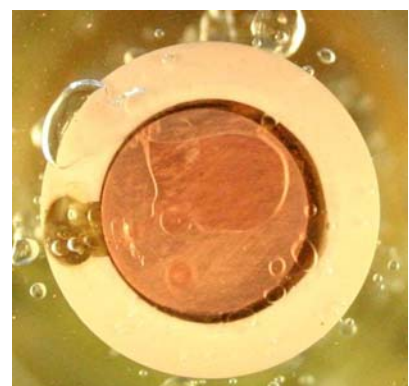
Figures 4 and 5 show photographs for the distances of 0.2 and 0.5 mm as a function of the heat flux between 7 and 40 kW/m^2 . We can observe an increase in the dry area of the copper disk with an increase in the heat flux. For $s=0.2 \text{ mm}$, the wall temperature shows a high value when the



$T_w= 61.0^\circ\text{C}; q=7\text{kW/m}^2$



$T_w= 61.2^\circ\text{C}; q=10\text{kW/m}^2$

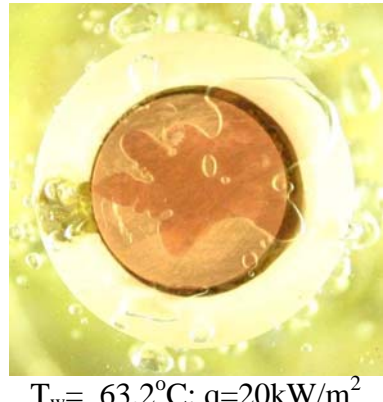


$T_w= 61.7^\circ\text{C}; q=12\text{kW/m}^2$

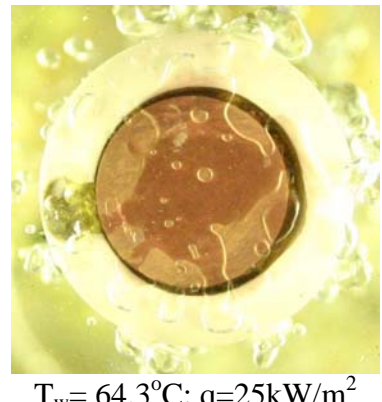
Figure 4. Effect of heat flux: confined boiling for $s=0.2 \text{ mm}$



$T_w = 62.3^\circ\text{C}$; $q = 15 \text{ kW/m}^2$



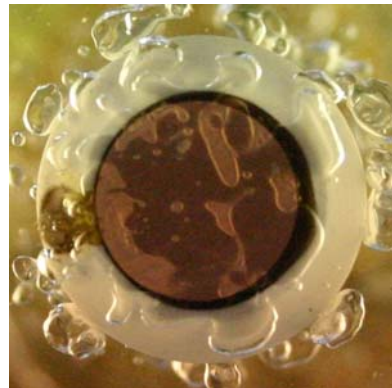
$T_w = 63.2^\circ\text{C}$; $q = 20 \text{ kW/m}^2$



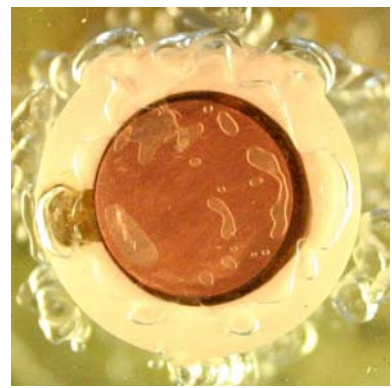
$T_w = 64.3^\circ\text{C}$; $q = 25 \text{ kW/m}^2$



$T_w = 65.9^\circ\text{C}$; $q = 30 \text{ kW/m}^2$

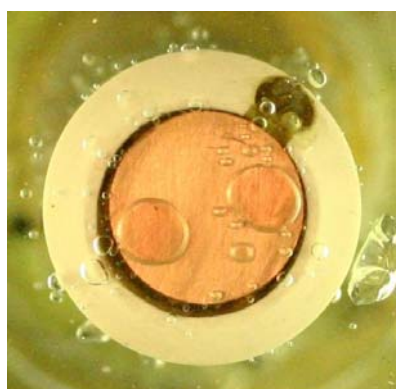


$T_w = 68.5^\circ\text{C}$; $q = 35 \text{ kW/m}^2$

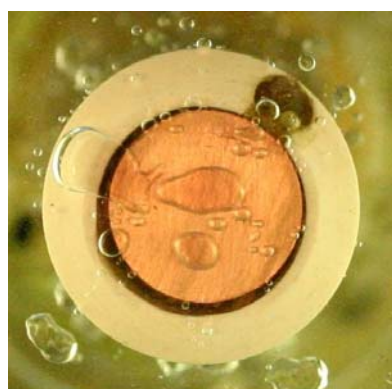


$T_w = 74.7^\circ\text{C}$; $q = 40 \text{ kW/m}^2$

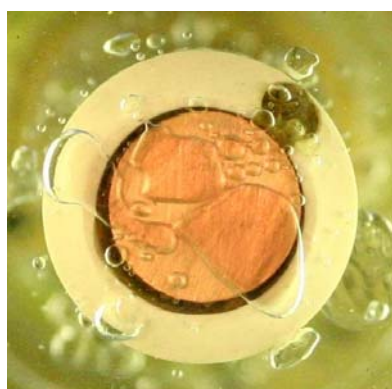
Figure 4. Effect of heat flux: confined boiling for $s=0.2 \text{ mm}$ (cont.)



$T_w = 63.4^\circ\text{C}$; $q = 7 \text{ kW/m}^2$

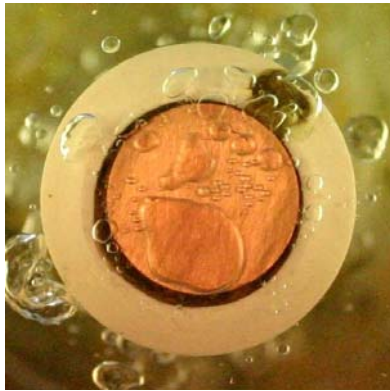


$T_w = 62.8^\circ\text{C}$; $q = 10 \text{ kW/m}^2$

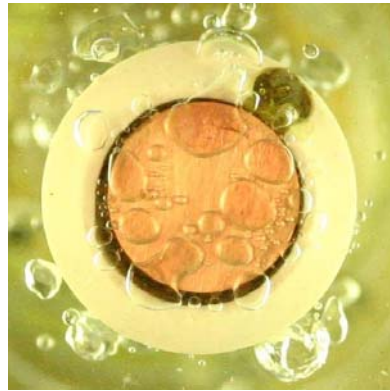


$T_w = 63.1^\circ\text{C}$; $q = 12 \text{ kW/m}^2$

Figure 5. Effect of heat flux: confined boiling for $s=0.5 \text{ mm}$



$$T_w = 63.6^\circ\text{C}; q = 15 \text{ kW/m}^2$$



$$T_w = 64.4^\circ\text{C}; q = 20 \text{ kW/m}^2$$



$$T_w = 65.3^\circ\text{C}; q = 25 \text{ kW/m}^2$$



$$T_w = 66.1^\circ\text{C}; q = 30 \text{ kW/m}^2$$



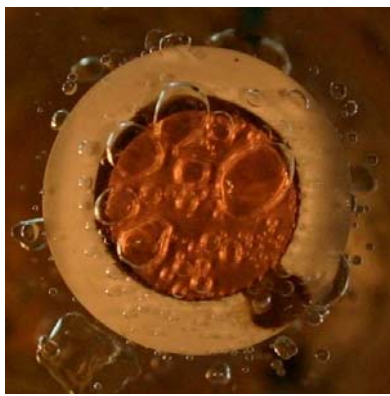
$$T_w = 67.1^\circ\text{C}; q = 35 \text{ kW/m}^2$$



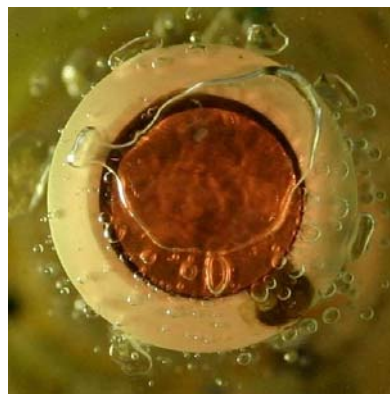
$$T_w = 68.1^\circ\text{C}; q = 40 \text{ kW/m}^2$$

Figure 5. Effect of heat flux: confined boiling for $s=0.5$ mm (cont.)

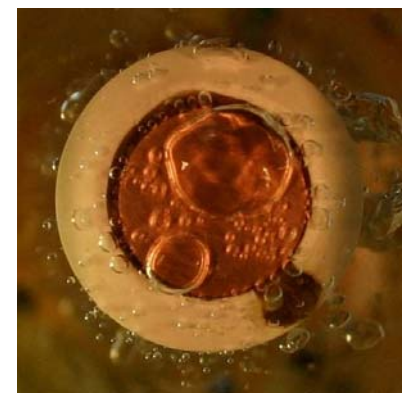
heat flux is 40 kW/m^2 , similar to that in Fig. 3c. Figure 5 shows that the increase in the dry area is followed by an increase in the wall temperature but without the significant increase observed in Fig. 4, for a heat flux of 40 kW/m^2 . The instabilities generated by bubbles escaping to the bulk liquid must cause the creation of a cold liquid front that allows the cooling of the copper disc without reaching a net dryout, except for the case with $s=0.2$ mm and a heat flux of 40 kW/m^2 . For $s=0.2$ and 0.5 mm the coalesced bubbles are deformed whereas for $s=1$ and 13 mm the coalesced bubbles are not so deformed.



$$T_w = 65.9^\circ\text{C}$$

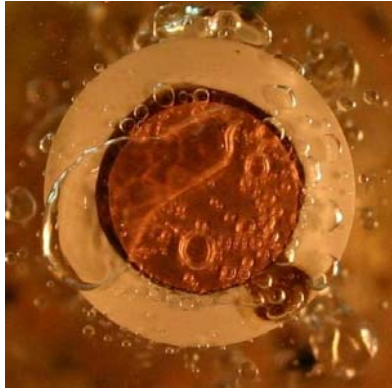


$$T_w = 65.9^\circ\text{C}$$

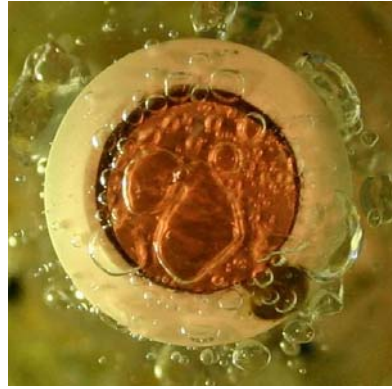


$$T_w = 65.8^\circ\text{C}$$

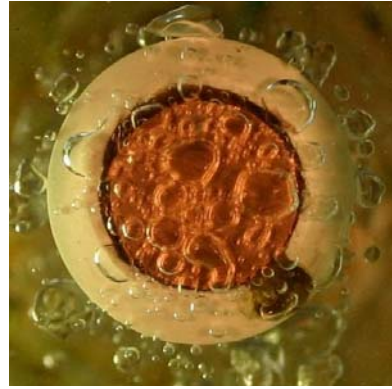
Figure 6a. $s=13$ mm; Heat flux of 20 kW/m^2



$T_w = 67.4^\circ\text{C}$

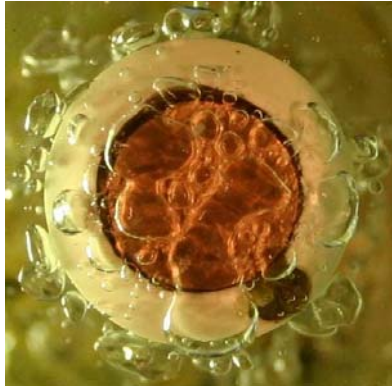


$T_w = 67.6^\circ\text{C}$

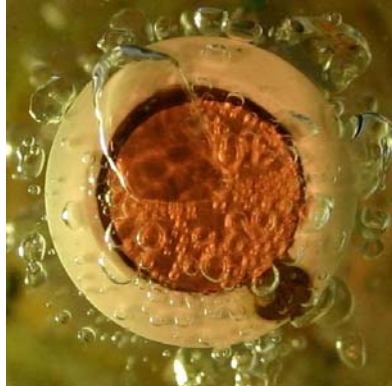


$T_w = 67.7^\circ\text{C}$

Figure 6b. $s=13$ mm; Heat flux of 30 kW/m^2



$T_w = 69.7^\circ\text{C}$



$T_w = 69.6^\circ\text{C}$



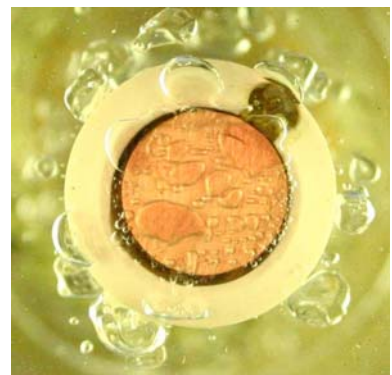
$T_w = 69.8^\circ\text{C}$

Figure 6c. $s=13$ mm; Heat flux of 40 kW/m^2

Figures 6a-c show different configurations without confinement for $s=13$ mm and three values of heat flux. The photographs show a great number of small bubbles and the presence of large bubbles escaping to the bulk liquid. A similar analysis was made for $s=0.5$ mm and heat flux of 30 kW/m^2 , Fig. 7, when the trend was the coalescence of the bubbles. Several photographs presented in this paper allow us to consider the strong effect of the escaping bubbles pumping vapour from the channel and causing a cold liquid front in the channel. This complex mechanism can be inferred from the photographs in Figs. 6a-c and Fig. 7, for $s=0.5$ mm. For 0.2 and 0.5 mm the photographs also show large coalesced bubbles escaping.



$T_w = 66.1^\circ\text{C}$



$T_w = 66.2^\circ\text{C}$



$T_w = 66.2^\circ\text{C}$

Figure 7. Confined boiling for $s=0.5$ mm and $q=30 \text{ kW/m}^2$

Figure 8 shows the corresponding partial boiling curve for distances s of 0.2, 0.5, 1 and 13 mm. For heat fluxes between 5 and 30 kW/m^2 the curves corresponding to $s=0.2$ and 0.5 mm are shifted to the left compared with the curves for $s=1$ and 13 mm, indicating an enhancement of the boiling heat transfer. For $s=0.2$ and a heat flux higher than 25 kW/m^2 a decrease in heat transfer occurs as is observed by the increase of the copper disc temperature and the corresponding increase of the dry area as shown in Fig. 3a-c. Particularly, for this latter case the wall temperature was higher than the value measured under the conditions in photograph 3-c.

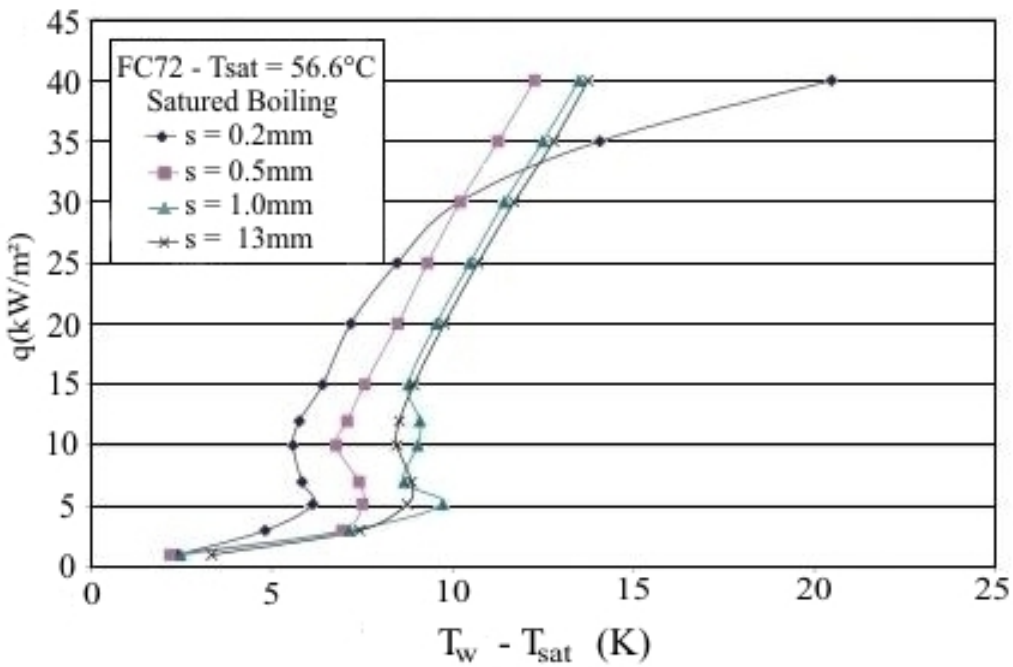


Figure 8. Partial boiling curves as a function of the distance s

4. CONCLUSIONS

Boiling in the narrow channel for $s=0.2$ ($Bo=0.28$) and 0.5 mm ($Bo=0.69$) resulted in few small bubbles and some coalesced and deformed bubbles. In contrast, for $s=1$ ($Bo=1.38$) and 13 mm ($Bo=17.95$) the heating copper disk is covered by small bubbles with the trend towards large coalesced bubbles escaping and slipping over the small bubbles sometimes engulfing them. One explanation of the higher heat transfer coefficient for the situations where $s=0.2$ and 0.5 mm is the evaporation of a liquid film between the deformed coalesced bubble and the wall. However the main cause of this relatively high heat transfer mechanism can be attributed to the strong effect of the large bubbles escaping which promotes a cold liquid front in the channel and the pulsating movement of the bubbles before departing from the channel. This mechanism is highly dependent on the particularly boundary conditions imposed by the geometrical characteristics of the heating disk and its support. The diameter of the latter can influence the residence time of the vapour mass in the channel.

5. ACKNOWLEDGEMENTS

The authors are grateful for the support of the Brazilian Space Agency (AEB), the INPE, the Research Council of Brazil (CNPq), the PROF Program of CAPES, and the Science and

Technology Foundation of Santa Catarina (FUNCITEC) in performing this study. The authors extend their thanks to 3M (Italy) for the donation of FC72.

6. REFERENCES

Bonjour, J. and Lallemand, M., 1997, "Effects of Confinement and Pressure on Critical Heat Flux During Natural Convective Boiling in Vertical Channels", *Int. Comm. Heat Mass Transfer*, Vol. 24 (2), pp. 191-200.

Carey, V.P., 1992, "Liquid-Vapor Phase-Change Phenomena", Taylor & Francis.

Dhir, V.K., 1996, "Pool Boiling Heat Transfer: Recent Advances and Expectations for the Future", in., *Process, Enhanced, and Multiphase Heat Transfer: A Festschrift for A. Bergles*, ed., R.M. Manglik and A.D. Kraus, Begell House, Inc., pp. 99-125.

Geisler, K.J.L. and Bar-Cohen, A., 2003, "Nucleate Pool Boiling Heat Transfer in Narrow Vertical Channels", *Proceedings of the 5th Int. Conference on Boiling Heat Transfer*, Session XII, Montego Bay, Jamaica, University of Florida, 5p.

Holman, J.P., 1989, "Experimental Methods for Engineers", McGraw-Hill, 5th ed.

Ishibashi, E. and Nishikawa, K., 1969, "Saturated Boiling Heat Transfer in Narrow Spaces", *Int. J. Heat Mass Transfer*, Vol. 12, pp. 863-894.

Katto, Y., Yokoya, S. and Teraoka, K., 1977, "Nucleate and Transition Boiling in a Narrow Space Between Two Horizontal, Parallel Disk Surfaces", *Bull. JSME*, Vol. 20, 143, pp. 638-643.

Kline, S.J., 1985, "The Purposes of Uncertainty Analysis", *ASME-Journal of Fluid Engineering*, Vol. 107, pp. 153-160.

Nowell Jr., R.M., Bhavnani, S.H. and Jaeger, R.C., 1995, "Effect of Channel Width on Pool Boiling from a Microconfigured Heat Sink", *IEEE Transactions on Components, Packaging, and Manufacturing Technology – Part A*, Vol. 18, N° 3, pp. 534-539.

Passos, J.C., Hirata, F.R., Possamai, 2004a, "Confined and Unconfined Nucleate Boiling on Downward Facing Surfaces", *4th European Thermal Science Conference*, Birmingham, UK, 28-31 March, pp. 1-13.

Passos, J.C., Hirata, F.R., Possamai, L.F.B., Balsamo, M. and Misale, M., 2004b, Confined Boiling of FC72 and FC87 on a Downward Facing Heating Copper Disk", *International Journal of Heat and Fluid Flow*, Elsevier, Vol. 25, issue 2, April, pp.313-319.

Passos, J.C. and Reinaldo, R. F., 2000, "Analysis of pool boiling within smooth and grooved tubes", *ETFS -Experimental Thermal and Fluid Science*, Elsevier, Vol. 22, pp. 35-44.

Séméria, R., 1964, "Analyse Fine de l'Ébullition à l'Échelle local", *Les Instabilités en Hydraulique et en Mécanique des Fluides*, VIIIèmes Journées de l'Hydraulique, Société Hydrodynamique de France-Lille-France, Question Vc, Rapport n° 1, pp. 1-7.

Stephan, K., 1992, "Heat Transfer in Condensation and Boiling", Springer-Verlag.

Yao, S.C. and Chang, Y., 1983, "Pool Boiling Heat Transfer in a Confined Space", *Int. J. Heat Mass Transfer*, Vol. 26 (6), pp. 841-848.